Atypical U3 snoRNA Suppresses the Process of Pterygium Through Modulating 18S Ribosomal RNA Synthesis

Xin Zhang,[1] Yaping Jiang,[1] Qian Wang,[2] Weishu An,[2] Xiaoyan Zhang,[3] Ming Xu,[2] and Yihui Chen[1]

[1]Department of Ophthalmology, Yangpu Hospital, School of Medicine, Tongji University, Shanghai, China
[2]Department of Oncology, Shanghai Ninth People's Hospital, Shanghai Jiao Tong University School of Medicine, Shanghai, China
[3]Department of Ophthalmology, Huashan Hospital, Fudan University, Shanghai, China

Correspondence: Yihui Chen, Department of Ophthalmology, Yangpu Hospital, School of Medicine, Tongji University, 450 Tengyue Road, Shanghai 200090, China; 1300089@tongji.edu.cn.
Ming Xu, Department of Oncology, Shanghai Ninth People's Hospital, Shanghai Jiao Tong University School of Medicine, 280 Mohe Road, Shanghai 201900, China; mingxu.msu@gmail.com.

XZ and YJ contributed equally to this article.

Received: January 8, 2022
Accepted: April 12, 2022
Published: April 26, 2022

Citation: Zhang X, Jiang Y, Wang Q, et al. Atypical U3 snoRNA suppresses the process of pterygium through modulating 18S ribosomal RNA synthesis. *Invest Ophthalmol Vis Sci.* 2022;63(4):17. https://doi.org/10.1167/iovs.63.4.17

Background. The progression and recurrence of pterygium mainly occur due to the abnormal proliferation and migration of stromal pterygium fibroblasts. This research explores the aberrant expression of small nucleolar RNA U3 (U3 snoRNA) in pterygium and elucidates the molecular mechanisms of U3 snoRNA in pterygium development.

Methods. Primary human conjunctival fibroblasts (HCFs) and human pterygium fibroblasts (HPFs) were separated and cultured from fresh conjunctiva grafts and pterygium tissues. The PLKO.1 lentiviral system and CRISPR/Cas9 recombinant construct were, respectively, used to overexpress and silence U3 snoRNA in HPFs and HCFs for further specific phenotype analysis. RNA-seq and TMT-labeled quantitative protein mass spectrometry were utilized to evaluate the effect of U3 snoRNA on mRNA transcripts and protein synthesis.

Results. Reduced U3 snoRNA in pterygium promotes HCF or HPF cells' proliferation, migration, and cell cycle but has no significant effect on apoptosis. U3 snoRNA modulates 18S rRNA synthesis through shearing precursor ribosomal RNA 47S rRNA at the 5′ external transcribed spacer (5′ ETS). Moreover, the altered U3 snoRNA causes mRNA and protein differential expression in HCF or HPF cells.

Conclusions. The atypical U3 snoRNA regulates the translation of specific proteins to exert a suppressive function in pterygium through modulating the 18S rRNA synthesis. Here, we uncover a novel insight into U3 snoRNA biology in the development of pterygium.

Keywords: small nucleolar RNA U3 (U3 snoRNA), pterygium, ribosome biosynthesis, 18S ribosomal RNA (18S rRNA)

Pterygium is a prevalent ocular surface disease that manifests as an invasion of the normal corneal epithelium by a proliferation of fibrovascular tissue on the conjunctiva,[1] which may cause corneal flashes and severe vision loss as the disease progresses.[2,3] A meta-analysis showed that the global prevalence of pterygium was 12%, with the highest majority of 53% in China.[4] Current treatment for pterygium is mainly surgical resection; however, the recurrence rate after surgery is still high (38%–88%).[5] Although improved surgical approaches with various adjuvant treatments have reduced the recurrence rate, recurrence persists from 3% to 40.9%.[6] Previous studies have revealed that heredity, fibrovascular proliferation and migration, anti-apoptosis, oxidative stress, extracellular matrix remodeling, and corneal stem cell dysfunction are implicated in pterygium pathogenesis.[7,8] Heredity factors, such as the genetics of P53 gene mutations, deletions,[9,10] and epigenetics (including DNA methylation modification, histone modification, and noncoding RNA regulations) are emerging as the crucial mechanisms in pterygium.[11–13]

Protein synthesis is an essential process for cell growth and development. The synthesis process requires a combination of ribosomes, translation factors, and tRNAs; however, dysregulation of protein translation may lead to cancer and other diseases.[14] In ribosome biosynthesis, precise regulation of the synthesis and assembly of its components occurs, with rRNA maturation being one of the most crucial steps.[15] Furthermore, 18S ribosomal RNA (18S rRNA) is the main constituent of the small 40S subunit of the ribosome. In mammalian cells, rDNA is transcribed by RNA polymerase I (Pol I) to produce the human precursor rRNA (47S rRNA), which then undergoes shearing, site-specific modifications (small nucleolar RNA [snoRNA]-mediated pseudouridine [ψ] and 2′-O-methyl ribose [2′ Ome]) to process into mature 18S, 5.8S, and 28S rRNA.[16] In addition, certain snoRNAs, such as U3, U8, and U14, are crucial in the regulation and maturation of rRNA.[17]

SnoRNA is a noncoding RNA that consists of 60 to 300 nucleotides and mainly accumulates in the nucleolus.[18] Based on the conserved sequence elements, snoRNAs can

be classified as C/D box or H/ACA box snoRNAs. C/D box snoRNAs contain two sequence motifs (C box = TGATGA and D box = CTGA) and direct 2′-O-methylation (2′ Ome) modifications of rRNA or snRNA.[19,20] H/ACA box snoRNAs contain two sequence motifs (H box = ANANNA and ACA box = ACA) and pseudouridylates the target RNA for modification.[21] Small nucleolar RNA U3 (U3 snoRNA), a specific C/D box snoRNA, contains box C′, B, C, and box D, is mainly involved in the maturation of 18S rRNA and the shearing of the 5′ external transcribed spacer (5′ ETS) of 47S rRNA in humans, thereby facilitating the process of ribosome biosynthesis.[22,23] However, whether U3 snoRNA was involved in the pathogenesis of pterygium remains to be elucidated. Our previous studies reported that atypical U3 snoRNA (Ensembl ID: ENSG00000212195) expression in pterygium tissues was significantly lower than that in conjunctiva tissues.[24] Therefore, in this present study, we aimed to investigate the association between decreased U3 snoRNA and the occurrence of pterygium. We verified the expression and related functions of U3 snoRNA, and highlighted the relationship among U3 snoRNA and rRNA, ribosome synthesis, and protein translation in the development of pterygium.

Materials and Methods

Specimen Collection

In total, 23 patients with pterygium (mean age = 55.9 ± 6 years) were included in this study and were observed in the Ophthalmology Department of Yangpu Hospital, Tongji University. All patients were diagnosed with grade III or higher pterygium and underwent pterygium excision and autologous conjunctiva transplantation. The criteria for grading the severity of pterygium were as described in previous studies.[25] Pterygium tissues and a small piece of normal conjunctiva tissue from an autograft at the contralateral corneal limbus were surgically obtained from one patient. Patients with other ocular diseases and/or those who underwent ophthalmic surgery were excluded from the study. This study was approved by the ethical committee of Yangpu Hospital, Tongji University, and conducted according to the principles of the Declaration of Helsinki. Written informed consent was obtained from all patients, and the surgically resected specimens were appropriately processed or preserved for quantitative reverse transcription PCR (RT-qPCR), primary cell culture, and in situ hybridization. The clinical information from 23 patients with pterygium was summarized in Supplementary Table S1.

Prepare Primary Human Conjunctival Fibroblasts and Pterygium Fibroblasts

All surgically removed fresh tissues were washed thrice with phosphate-buffered saline (PBS) and cut into small pieces (1–2 mm in diameter) under an ophthalmic microscope. Tissue blocks were incubated with Dulbecco's Modified Eagle Medium/Nutrient Mixture F-12 (DMEM/F12) medium supplemented with 10% fetal bovine serum, 100 U/mL penicillin, and 100 mg /mL streptomycin (materials originated from Gibco Life Technologies, Shanghai, China) in an incubator (37°C and 5% CO_2). After 3 to 4 days of culture, fibroblasts migrated out from the edge of the explants and exhibited a typical spindle-shaped morphology. The medium was changed thrice per week after cell growth appeared in the explants. Moreover, when a sufficient number of fibroblasts were obtained around each explant, the passaged cultures were digested with trypsin-ethylenediaminetetraacetic acid (EDTA; 0.25%; Gibco Life Technologies, Shanghai, China) at 37°C and 5% CO_2 for 3 to 4 minutes (the digestion time of cell passages was approximately 2 minutes). Cells from the third to the seventh generation were used for the experiments described in this report.

Plasmids

The pLKO.1 vector with puromycin resistance (SHC001; Sigma-Aldrich) was selected for lentivirus-mediated overexpression U3 snoRNA.[26] The nested PCR amplified the full-length sequence of overexpressed U3 snoRNA. The complete U3 snoRNA was amplified using two pairs of PCR primers; U3 snoRNA-F1: TGTGTGAGTTTCTTTCGCATG and U3 snoRNA-R1: ACTACTCAGACTGCCTTCTC, U3 snoRNA-F2: TGGAAAGGACGAAACACCGGTAAGACTATATTTTGAGGGA, and U3 snoRNA-R2: CTCGAGGTCGAGAATTCACTACTCAGACTGCCTTCTC. The plasmid pSpCas9(BB)-2A-GFP (PX458), a gift from Feng Zhang (#48138; Addgene),[27] was used for silencing endogenous U3 snoRNA. Briefly, two small guide RNAs (sgRNAs), with the sequence of TATCTGAACGTGTAGAACGC or TGACCGTTCTTCTCTAGAGA, were inserted into the Bbs I sites in pSpCas9(BB)-2A-GFP. The two recombinant plasmids containing specific sgRNA were co-transfected into human conjunctival fibroblasts (HCFs) by Lipofectamine 3000 Transfection Reagent (L3000015; Thermo Fisher Scientific, Waltham, MA, USA). After 36 hours, the strongly GFP-positive cells were screened by flow sorting and cultured for subsequent experiments. We meant to perform CRISPR to knockout U3 snoRNA in primary cultured human conjunctival fibroblasts; however, we failed to amplify individual positive cells for further investigations. Therefore, all the GFP-positive cells were collected and cultured with a similar effect to RNAi, termed CRISPRi in this work.

Antibodies

Antibodies Bax (#5023), Bcl_2 (#4223), D-type cyclins D1 (cyclin D1, #55506), D-type cyclins D3 (cyclin D3, #2936), cyclin-dependent kinase 4 (CDK4, #12790), cyclin-dependent kinase 6 (CDK6, #13331), P21 (# 2947), proliferating cell nuclear antigen (PCNA, #2586), and β-actin (#58169) were from Cell Signaling Technology. Antibody Ki67 (sc-23900) was from Santa Cruz Biotechnology.

Immunofluorescence

HCFs and human pterygium fibroblasts (HPFs) were fixed in 4% paraformaldehyde (P0099, Beyotime, Peking, China), permeabilized with 0.5% Triton X-100 (T9284; Sigma-Aldrich, PBS-Tween dilution), and blocked with 5% bovine serum albumin (BSA; Sigma-Aldrich) for 30 minutes at room temperature. After washing thrice with PBS, primary antibodies against vimentin (Santa Cruz Biotechnology; 1:150, cat. no. SC6260) and cytokeratin (Santa Cruz Biotechnology; 1:150, cat. no. SC58719) were diluted with 1% BSA and blocked overnight at 4°C. After that, the samples were washed thrice with PBS and incubated with Alexa Fluor 488-labeled and 568-labeled secondary antibodies (A12379 and A11011; Thermo Fisher Scientific) at 1:200 dilutions for 2 hours at room temperature and protected from light. Next, the nuclei were labeled with 4′, 6-diamidino-2-phenylindole

Investigative Ophthalmology & Visual Science

for 15 minutes, and the samples were washed thrice with PBS. Eventually, images were captured under a fluorescence microscope (Olympus, Tokyo, Japan).

Quantitative Reverse Transcription-PCR

According to the manufacturer's instructions, total RNA was isolated from 16 pterygium tissues and paired with normal conjunctiva tissues. The RNA quantity and quality were measured using NanoDrop 2000 (Thermo Fisher Scientific). RNA integrity was assessed using standard denaturing agarose gel electrophoresis. According to the manufacturer's protocol, total RNA was reverse transcribed to cDNA using a PrimeScript RT reagent kit with gDNA Eraser (RR047A; TaKaRa, Japan). The StepOnePlus real-time PCR detection system (Thermo Fisher Scientific) analyzed the RNA transcript levels. All samples were normalized to U6. The primers used for RT-qPCR are listed in Supplementary Table S2.

Wound Healing Assay

In this assay, 2×10^5 cells/well of HPFs overexpressing U3 snoRNA and HCFs knocking down U3 snoRNA were seeded into a 6-well plate. When the cells reached confluence, we performed serum-free starvation culture for 8 hours, and the monolayer was scratched and washed with PBS, followed by serum-free DMEM/F12. After that, the images were captured at 0, 24, and 48 hours after scratching. The scratch area was calculated using the ImageJ software (National Institutes of Health, Bethesda, MD, USA). The 24 hour scratch area ratio to the 0 hour scratch area was compared between the control and experimental groups.

Western Blotting

Cells were washed thrice with ice-cold PBS and lysed for 1 minute with 1.5% SDS lysis buffer (10 mM Tris-HCl [pH 7.4], 2 mM EDTA, and 1.5% SDS) supplemented with 1 mM phenylmethanesulfonyl fluoride (PMSF; ST505; Beyotime, Peking, China). After that, the cells were scraped off and collected into 1.5 mL EP tubes, sonicated, and incubated in a metal bath at 100°C for 10 minutes. The supernatant was collected via centrifugation at 12,000 rpm for 15 minutes, and the proteins were quantified using a BCA Protein Quantification Kit (P0012;, Beyotime). Equal amounts of protein were sampled and separated by SDS-PAGE and then transferred onto PVDF membranes (Millipore, Darmstadt, Germany). After incubation with specific antibodies, the signals of the detected proteins were visualized with enhanced chemiluminescence (Millipore, MA, USA) and captured using the ChemiDoc imaging system (BioRad, Hercules, CA, USA).

In Situ Hybridization

Three pairs of fresh conjunctiva and pterygium tissues were sliced after paraffin embedding. The slides were deparaffinized with xylene and gradient ethanol and washed with DEPC water. After digestion with protein K (20 ug/mL) at 37°C for 20 to 30 minutes, the slides were incubated for 1 hour in a pre-hybridized solution and hybridized with digoxigenin (DIG)-labeled U3 snoRNA probes at 37°C in a thermostat overnight. After hybridization, mouse anti-digoxigenin-labeled alkaline phosphatase (anti-DIG-AP) was added dropwise. Eventually, nitro blue tetrazolium chloride monohydrate (NBT) and nuclear solid red were used for staining. The sections were then sealed for image acquisition and analysis.

Data Analysis

All RT-qPCR experiments were set in triplicate and performed at least three times, and other presented experiments were performed at least three times. Statistical analyses were performed using the SPSS software (version 25.0., Cary, NC, USA) and GraphPad Prism software 7.0 (GraphPad Software, San Diego, CA, USA). The data were analyzed for normal distribution before the statistical analysis. Values are presented as mean ± standard deviation (SD). The student's *t*-test was used for normally distributed data, and nonparametric tests were used for abnormal distributions. Statistical significance was set at $P < 0.05$. Statistical significance is indicated as follows: $^{*}P < 0.05$, $^{**}P < 0.01$, $^{***}P < 0.001$, and $^{****}P < 0.0001$.

Results

U3 snoRNA Expression is Decreased in Pterygium

In our previous transcriptional profiling studies, we identified a series of genes and pathways in pterygium and found that several interesting noncoding RNAs were differentially expressed between conjunctiva and pterygium tissues.[24] Therefore, we extracted and analyzed the data on these noncoding RNAs. We found that U3 snoRNA was the most variable of these noncoding RNAs, with a log2fold change ([log2FC] = −4.33, $P < 0.0001$), and was expressed much less in the pterygium tissues (Figs. 1A, 1B). The 26 differentially expressed noncoding RNAs are listed in Table 1. Moreover, we quantified U3 snoRNA levels and examined the localization of U3 snoRNA in the pterygium and normal conjunctiva tissues via in situ hybridization (ISH). It was observed that U3 snoRNA expression in pterygium tissues was markedly suppressed than that in normal conjunctiva tissues (Fig. 1C). The results of ISH and IHC showed that U3 snoRNA and proliferation-associated indicator Ki67 exhibited opposite expression trends, and ISH also revealed U3 snoRNA was mainly expressed in stromal fibroblasts and basal epithelial cells (Fig. 1D). Therefore, we suggest that reduced U3 snoRNA in pterygium tissues may be associated with pterygium development.

The Primary HPFs and HCFs Were Successfully Separated, Identified, and Compared on the U3 snoRNA Expression

To understand the expression and functional mechanism of U3 snoRNA in cells, we conducted primary cultures of HCFs and HPFs, and details are depicted in Figure 2A. To characterize the cultured HCFs and HPFs, we detected the expression of vimentin-positive and cytokeratin-negative in fibroblasts by the immunofluorescence staining. HeLa cells were set as the control cells of the epithelium with positive cytokeratin staining (Fig. 2B). According to the RT-qPCR analysis, U3 snoRNA expression was significantly lower in HPFs than HCFs, consistent with that in tissues (Fig. 2C). As reported, specific cytokines and UV light can induce the occurrence and development of pterygium.[28] We exposed the HCFs to the different intensities of UV light (100, 200 mJ/cm^2) and concentrations of TGF-β (10, 20, 40 ng/ml) to examine

Investigative Ophthalmology & Visual Science

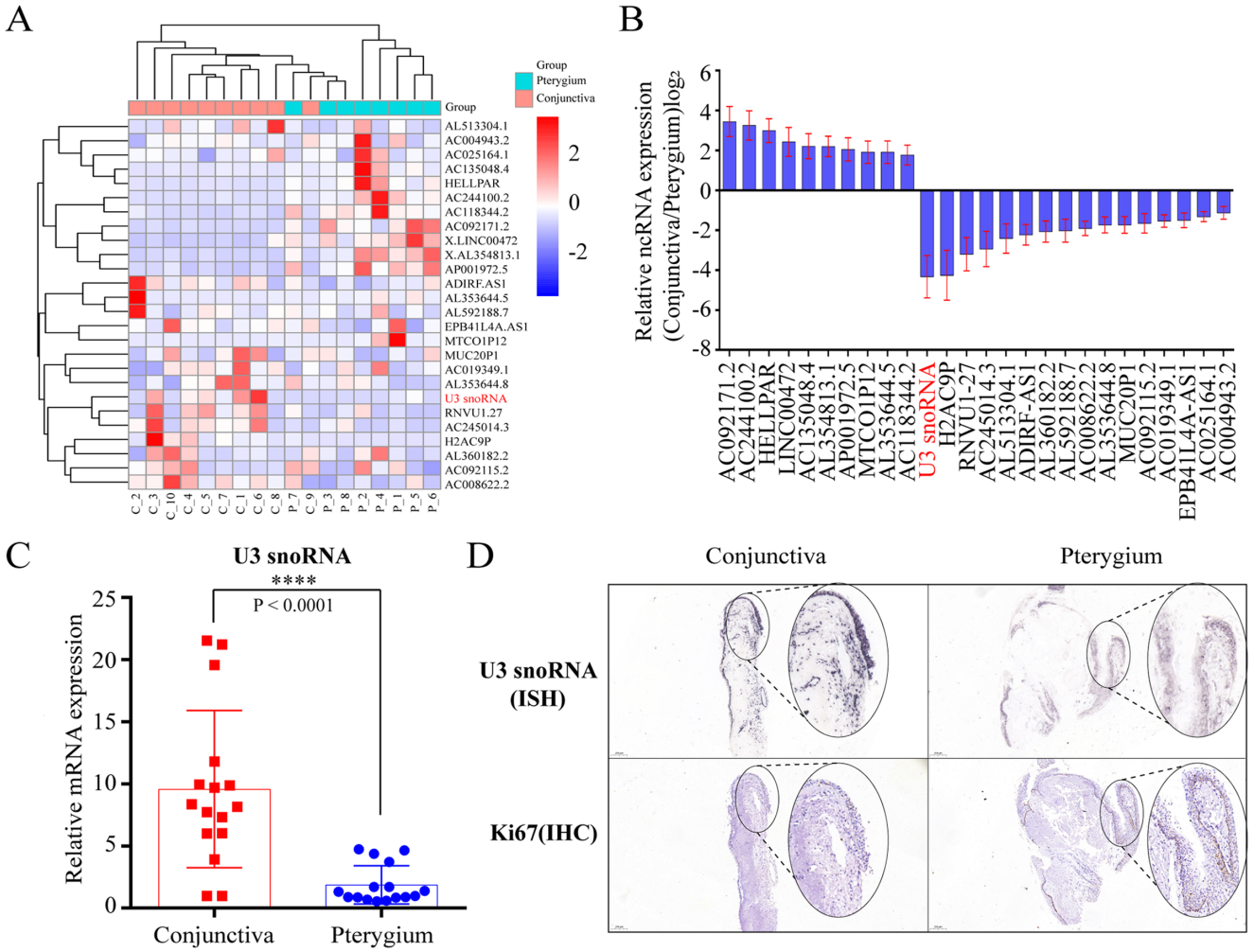

Figure 1. U3 snoRNA expression is decreased in pterygium. (**A**) Heatmap of 26 differentially expressed noncoding RNAs in pterygium transcriptomics analysis (C: conjunctiva, $n = 10$; P: pterygium, $n = 8$). (**B**) U3 snoRNA is the most significantly differentially expressed of 26 noncoding RNAs. (**C**) Expression of U3 snoRNA was measured via RT-qPCR in 16 pairs of normal conjunctiva and pterygium tissues ($n = 16$). (**D**) in situ hybridization revealed the distribution and differential expression of U3 snoRNA in normal conjunctiva and pterygium tissues, and immunohistochemical staining showed the expression of Ki67 in normal conjunctiva and pterygium tissues ($n = 3$). $^{*}P < 0.05$, $^{**}P < 0.01$, $^{***}P < 0.001$, and $^{****}P < 0.0001$.

the expression alteration of U3 snoRNA. Surprisingly, U3 snoRNA was significantly downregulated in the HCFs subjected to UV light or TGF-β treatment compared with untreated HCF cells (Fig. 2D). Together, we successfully separated and validated the primary cells of HPF and HCF, which could be used further to investigate the biological function of U3 snoRNA in pterygium.

U3 snoRNA Suppresses the Proliferation and Migration of HPF Cells

To explore the biological function of U3 snoRNA in HCFs and HPFs, we overexpressed U3 snoRNA in the HPF cells using the PLKO.1 lentiviral system and silenced U3 snoRNA in HCF cells using the CRISPR/Cas9 system (Figs. 3A, 3B). Increased U3 snoRNA significantly inhibited the capabilities of HPF cell proliferation (Fig. 3C) and migration (Fig. 3E). In contrast, U3 snoRNA-knocking down in HCFs promoted the relevant cell phenotypes (Figs. 3D, 3F). In addition, the expression of proliferating cell nuclear antigen (PCNA) yielded consistent outcomes that U3 snoRNA could suppress the cell proliferation in pterygium according to the western-blot analysis (Supplementary Fig. S1A). These results indicated that U3 snoRNA is involved in developing pterygium, at least in cell growth and cell mobility.

U3 snoRNA Mainly Causes G0/G1 Phase Arrest, But Not Apoptosis in HPF Cells

To assess whether U3 snoRNA-associated cell proliferation is related to apoptosis, we analyzed the apoptosis ability of HPF cells with or without U3 snoRNA expression by the flow cytometric method. Unfortunately, no significant variation (sum of early apoptosis and late apoptosis cells) was observed in normal or UV-treated HPF cells upon U3 snoRNA expression (Figs. 4A, 4B). However, overexpressed U3 snoRNA in HPFs or silenced U3 snoRNA in HCFs respectively arrested or facilitated the cell cycle in the G0/G1 phase (Figs. 4C, 4D), which is supposed to be closely associated with the cell proliferation capability.[29]

Investigative Ophthalmology & Visual Science

Table 1. Transcriptomics Analysis of 26 Differentially Expressed Noncoding RNAs

Gene ID	Gene Name	Symbol	Type	Base Mean	log2Fold Change	Regulation	*P* Value	*P* adj
ENSG00000230733	AC092171.2	lncRNA	NA	4.872414064	3.44120253	up	0.00000487	0.001145538
ENSG00000233237	LINC00472	lncRNA	NA	3.745425383	2.425835622	up	0.000820623	0.042689045
ENSG00000237973	MTCO1P12	Unprocessed pseudogene	NA	22.73479356	1.908951494	up	0.000645373	0.036565528
ENSG00000255438	AL354813.1	lncRNA	NA	10.2762454	2.196738839	up	0.0000179	0.00293655
ENSG00000275431	AC244100.2	lncRNA	NA	4.546910002	3.249354381	up	0.0000101	0.00187793
ENSG00000275684	AL353644.5	Novel miRNA	NA	70.19880738	1.907936744	up	0.000809433	0.042683752
ENSG00000279117	AP001972.5	TEC	NA	4.671328122	2.052222096	up	0.000419397	0.028701683
ENSG00000279196	AC135048.4	TEC	NA	6.206293012	2.206597952	up	0.000460306	0.030160806
ENSG00000279759	AC118344.2	TEC	NA	7.405720813	1.762637902	up	0.000370759	0.026553234
ENSG00000281344	HELLPAR	lncRNA	NA	7.589127505	2.987183413	up	0.000000639	0.000228769
ENSG00000212195	U3	snoRNA	NA	3.228619073	-4.332995704	down	0.0000429	0.005795848
ENSG00000218281	H2AC9P	Unprocessed pseudogene	NA	1.964733629	-4.259420698	down	0.000665138	0.03714885
ENSG00000224032	EPB41L4A-AS1	lncRNA	NA	26.53611127	-1.503206452	down	0.0000332	0.004819844
ENSG00000224769	MUC20P1	Unprocessed pseudogene	NA	21.47735097	-1.733404298	down	0.0000351	0.005001856
ENSG00000228417	AL360182.2	lncRNA	NA	5.821310348	-2.067415875	down	0.000098	0.01093765
ENSG00000229732	AC019349.1	lncRNA	NA	892.2293645	-1.541518886	down	0.000000571	0.000219712
ENSG00000233052	AL513304.1	lncRNA	NA	8.35074879	-2.419424699	down	0.00097987	0.046712191
ENSG00000245904	AC025164.1	lncRNA	NA	80.63110854	-1.322286854	down	0.000000105	0.0000559
ENSG00000259768	AC004943.2	lncRNA	NA	13.98243126	-1.131414533	down	0.000429159	0.029239779
ENSG00000261602	AC092115.2	lncRNA	NA	9.913991879	-1.657078691	down	0.000622194	0.035967922
ENSG00000272734	ADIRF-AS1	lncRNA	NA	34.47461863	-2.230443225	down	0.0000169	0.002835918
ENSG00000274210	RNVU1-27	snRNA	NA	5.70071146	-3.204406227	down	0.000122924	0.012703289
ENSG00000275719	AC008622.2	lncRNA	NA	18.91827156	-1.911216119	down	8.87E-08	0.0000506
ENSG00000276216	AC245014.3	lncRNA	NA	2.823985747	-2.940035781	down	0.000860562	0.043969192
ENSG00000276402	AL353644.8	Novel miRNA	NA	207.3666711	-1.737381313	down	0.0000128	0.002338795
ENSG00000277145	AL592188.7	Novel miRNA	NA	6621.40686	-2.028523189	down	0.000406526	0.028179096

To confirm that, Western blot detection of apoptosis- and cell cycle-related proteins in the HPFs overexpressing U3 snoRNA and HCFs knocking down U3 snoRNA supported the flow-cytometric analysis (Figs. 4E–H). Taken together, we suggest that decreased U3 snoRNA in pterygium may enhance the development of pterygium by arresting the G0/G1 phase, which further enhances the cell proliferation ability of fibroblast cells.

U3 snoRNA Involves in the 47S rRNA Shearing and Maturation of 18S rRNA

Numerous studies have reported that U3 snoRNA is associated with the shearing of precursor rRNA (47S rRNA) and the synthesis of 18S rRNA.[30,31] Therefore, we performed a comprehensive analysis of the location, structure, and interaction sites of U3 snoRNA with 18S rRNA. The target U3 snoRNA is located in the intron of the host gene TEX14 on chromosome 17 (Fig. 5A). Compared with human U3 (X14945, M14061, and AF020531) in Rfam (http://rfam.xfam.org/), we found that the atypical U3 snoRNA was presented with the differential base clusters, termed C′ (AGGAAGA [typical] vs. AGAGGGA [atypical]), B (GAGCGTGAAG [typical] vs. GAGTGGGATA [atypical]), C box (TGATGA [typical] vs TGGTGA [atypical]; Fig. 5B). The secondary structure was plotted based on ENSG00000212195 in Ensembl (https://asia.ensembl.org/index.html; Fig. 5C). The complementary base pairing between U3 snoRNA and the 5′ ETS and 18S rRNA in 47S rRNA was determined by the CLUSTALW tool (https://www.genome.jp/tools-bin/clustalw). A high degree of base complementary pairing was found at the four positions (i.e. positions 3 to 21, 23 to 27, 39 to 48, and 63 to 72 in U3 snoRNA, respectively; Fig. 5D). To identify the variations of 47S rRNA upon U3 snoRNA expression status in pterygium cells, we first plotted the model of precursor rRNA (47S rRNA) shearing into mature 18S rRNA, 28S rRNA, and 5.8S rRNA (Fig. 5E, upper panel).[16,22] A serious of distinctive primers were designed to detect 5′ ETS and mature 18S rRNA, 28S rRNA, and 5.8S rRNA (Primers F′ + R′ for 47S rRNA detection, $F_1 + R_1$ for 47S and 45S rRNA, $F_{18p} + R_{18p}$, $F_{28p} + R_{28p}$, and $F_{5.8p} + R_{5.8p}$ for pre-18S, -28S, and -5.8S rRNA, and $F_{18} + R_{18}$, $F_{28} + R_{28}$, and $F_{5.8} + R_{5.8}$ for total 18S, 28S, and 5.8S rRNA; Fig. 5E, lower panel). By RT-qPCR analysis, we found that A′ and A0 were significantly downregulated in HPFs overexpressing U3 snoRNA and significantly increased in HCFs with silenced U3 snoRNA, suggesting that altered U3 snoRNA can cause 5′ ETS shearing of 47S rRNA (Fig. 5F). Meanwhile, 18S rRNA maturing was accelerated in HPFs overexpressing U3 snoRNA while delayed in HCFs with silenced U3 snoRNA (Fig. 5G). In addition, the generation of mature 28S was correspondingly accelerated with the enhanced shearing of mature 18S and vice versa (see Fig. 5G). Taken together, atypical U3 snoRNA in pterygium participates in the 47S rRNA shearing and 18S rRNA maturation, and even 28S rRNA generation.

U3 snoRNA Mainly Affects the Proteome Profile by Regulating the Ribosome Function in Pterygium

Because 18S rRNA and 28S RNA are the critical components of the ribosome, we performed mass spectrometry analysis to assess the biological significance of U3 snoRNA in pterygium. The differentially expressed proteins in HPF overexpressing U3 snoRNA or in HCFs with silenced U3 snoRNA were enriched and plotted as the Heatmaps compared to the proper control, respectively (Figs. 6A, 6B). The gene ontology (GO) analysis revealed that differentially expressed proteins are mainly involved in the single-organism process and biological regulation in both HPFs overexpressing U3 snoRNA and HCFs with silenced U3 snoRNA (Fig. 6C). After crossing analysis of two mass spectrometry datasets, we obtained eight potential proteins that may closely relate to the U3 snoRNA regulated translation process (Fig. 6D). To identify whether U3 snoRNA affects the transcription of genes, we performed RNA-seq for transcriptomic analysis

Investigative Ophthalmology & Visual Science

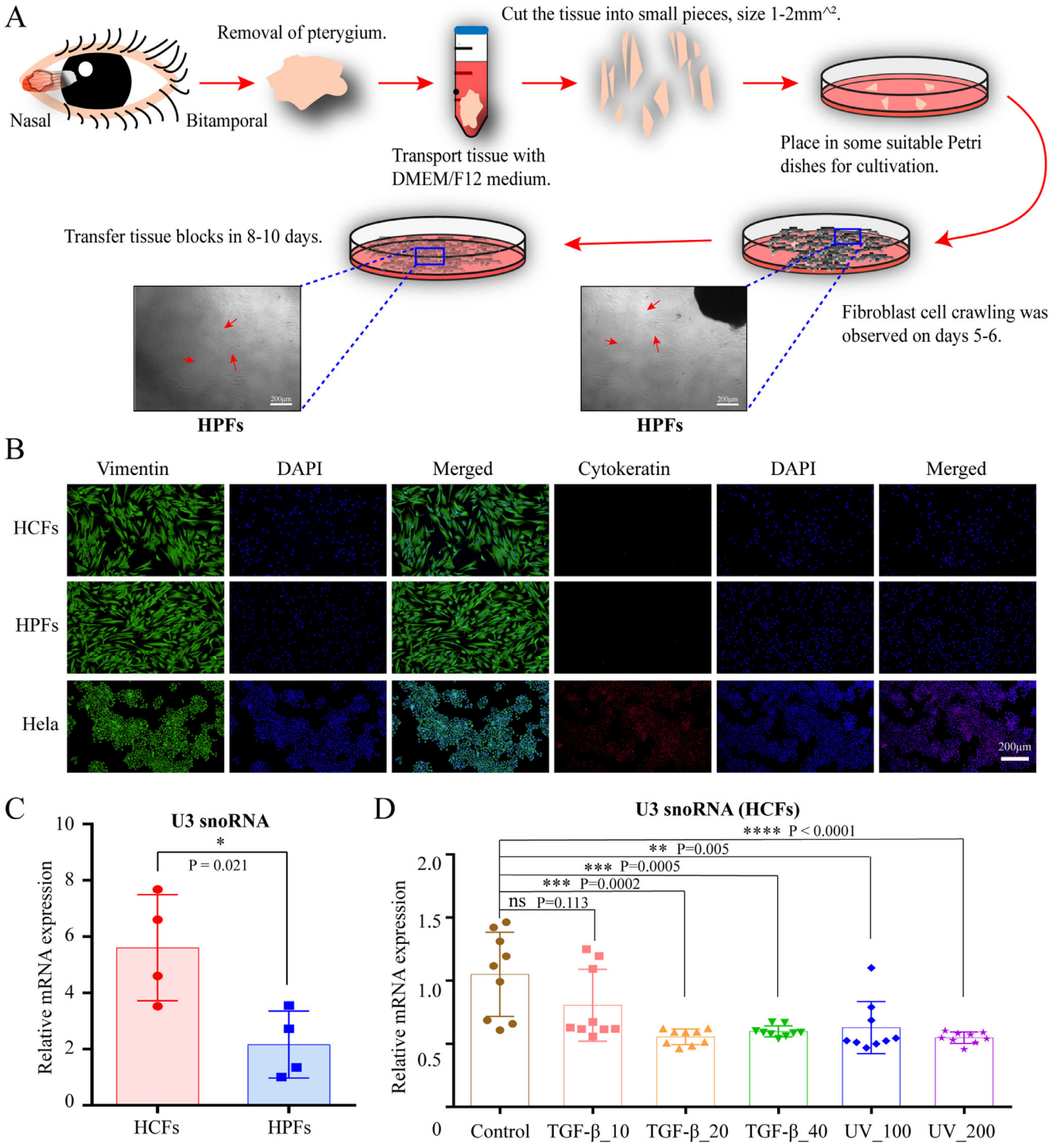

Figure 2. The primary HPFs and HCFs were successfully separated, identified, and compared on the U3 snoRNA expression. (**A**) Flow chart of primary cell culture. (**B**) Immunofluorescence of cytokeratin and vimentin expression in HCFs and HPFs (HeLa cells were set as the control cells of the epithelium with positive cytokeratin staining). (**C**) Expression of U3 snoRNA in four pairs of HCFs and HPFs were detected via RT-qPCR ($n = 4$). (**D**) The expression of U3 snoRNA in different doses of UV light (100, 200 mJ/cm^2) and TGF-β (10, 20, 40 ng/ml) induced HCFs was examined via RT-qPCR. *$P < 0.05$, **$P < 0.01$, ***$P < 0.001$, and ****$P < 0.0001$.

in HPFs overexpressing U3 snoRNA, and only 30 differentially expressed genes were found (upregulated 19 genes and downregulated 11 genes; Fig. 6E). GO and Kyoto Encyclopedia of Genes and Genomes (KEGG) pathway analyses revealed that differentially expressed genes were mainly enriched in growth and rhythmic processes (Supplementary Fig. S1B), involved in Wnt, cellular junctions, or proteoglycan signaling pathway (Fig. 6F). In addition, we did not find the mRNA expression change of any of the eight U3 snoRNA-associated proteins (Table 2). These implicated that

Investigative Ophthalmology & Visual Science

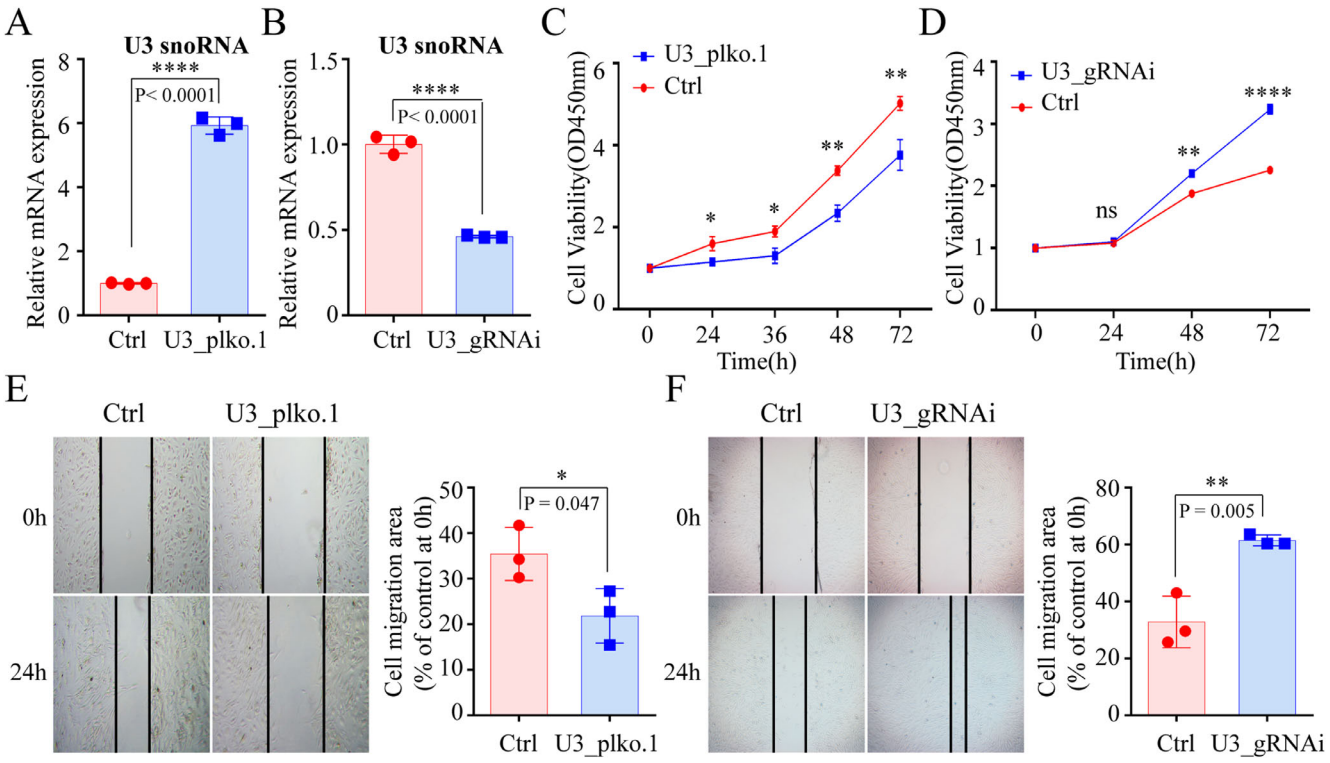

Figure 3. U3 snoRNA suppresses the proliferation and migration of HPFs. (**A, B**) Efficacy of overexpression and knocking down of U3 snoRNA by RT-qPCR. (**C, D**) CCK8 assays depicted that the overexpression or knocking down of U3 snoRNA inhibited or promoted cell proliferation, respectively. (**E, F**) Cell scratching revealed that the overexpression and knocking down of U3 snoRNA inhibited and promoted cell migration, respectively. *$P < 0.05$, **$P < 0.01$, ***$P < 0.001$, and ****$P < 0.0001$.

the alteration of the protein caused by U3 snoRNA probably, to a larger extent, due to the ribosome function but not the mRNA transcription. Together, U3 snoRNA in pterygium mainly affects the proteome profile in pterygium through shearing the 5′ ETS of 47S rRNA to promote 18S rRNA synthesis and ribosome function, which could be a novel mechanism of pterygium formation and growth (Fig. 7).

Discussion

Pterygium is a multifactorial disease. Chronic UV exposure is the predominant factor in pterygium development.[32] In addition, chronic inflammation and some ocular surface diseases (e.g. xerophthalmia) are also involved.[33,34] These environmental or self-induced factors can lead to conjunctival pathological changes, such as fibrosis, chronic inflammation, and extracellular matrix (ECM) remodeling.[35,36] Moreover, previous studies have shown that the recurrence of pterygium mainly stems from excessive proliferation of fibroblasts.[37] Therefore, we isolated and cultured the primary fibroblasts from patients for the functional observation of U3 snoRNA in pterygium development (see Figs. 2A–C). To identify the separated HPF or HCF cells, we found that U3 snoRNA was indeed significantly downregulated in HCFs subjected to UV irradiation and TGF-β treatment (Fig. 2D), which facilitated the investigation on the relationship between U3 snoRNA and the general etiology of pterygium.

Epigenetics is relevant to ocular diseases,[38,39] and noncoding RNA regulation, including microRNAs,[40] lncRNAs,[41] and circRNAs,[42] have been extensively studied in pterygium; however, studies on the mechanism of action of snoRNAs in pterygium development have not been reported. The snoRNAs, as a member of noncoding RNAs, are primarily involved in directing post-transcriptional modifications of rRNA and snRNA,[43] and U3 snoRNA is a specific C/D box snoRNA[17,44] that involved in rRNA processing.[45–47] When base-paired with pre-rRNA, this hairpin (folded from 5′ end of the U3 snoRNA) opens and interacts with different 5′ ETS and/or 18S rRNA, guiding the 5′ ETS shearing in human 47S rRNA (35S rRNA in yeast) and the maturation of 18S rRNA to mediate ribosome synthesis.[16] Shearing of the 5′ ETS is the most initial and critical step in rRNA maturation. The 5′ ETS in human precursor rRNA consists of three shearing sites, A′, A0, and A1, in which A′ is the first to be sheared (see Fig. 5E, upper panel).[48] Consistent with our study, we found that the sites in 5′ ETS where atypical U3 snoRNA (C′, B, and C boxes are differing from boxes of Rfam's U3 snoRNA) binds are all located within the A′ region (approximately -3654 bp to -3230 bp) and trigger 18S rRNA maturing (see Figs. 5E–G). Suppressed U3 snoRNA in pterygium attenuates the 5′ ETS shearing of 47S rRNA, which results in the maturation disorder of 18S rRNA, and even 28S rRNA (see Fig. 1 and Figs. 5F, 5G), thereby causing the deficiency of ribosome function to induce pterygium cell formation, proliferation, and migration (see Fig. 3).

Considering that, we analyzed the proteomic profile induced by U3 snoRNA regulation, and several interesting proteins were greeted (see Figs. 6A–D). Among them, the major facilitator superfamily domain containing 1 (MFSD1) is supposed to be the most relative to the U3 snoRNA

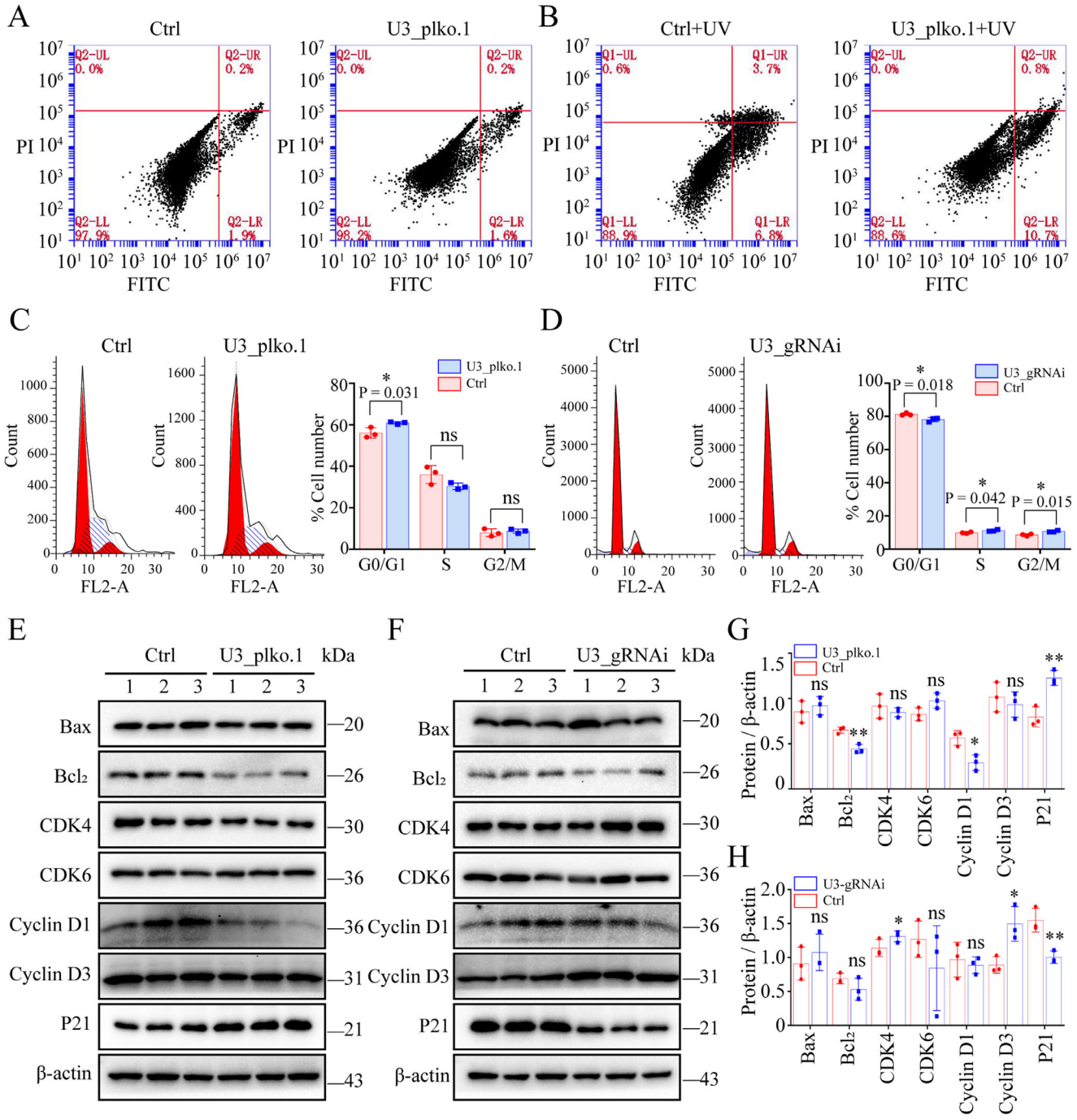

Figure 4. U3 snoRNA mainly causes G0/G1 phase arrest, but not apoptosis in HPFs. **(A)** Flow analysis revealed that the overexpression of U3 snoRNA did not affect apoptosis (LR + UR). **(B)** Flow analysis depicted that the overexpression of U3 snoRNA also did not affect apoptosis after UV induction (LR + UR). **(C)** HPFs overexpressing U3 snoRNA were blocked in G0/G1 phase. **(D)** HCFs knocking down U3 snoRNA facilitated the progression of HCFs from G0/G1 phase to S and G2/M phases. **(E, F)** The expression levels of apoptosis-related proteins (Bax, Bcl_2, CDK4, CDK6, Cyclin D1, Cyclin D3, and P21) were determined by Western blotting and the corresponding densitometric analysis results **(G, H)**. $^{*}P < 0.05$, $^{**}P < 0.01$, $^{***}P < 0.001$, and $^{****}P < 0.0001$.

regulation in pterygium because of the close correspondence between U3 snoRNA expression and ribosome synthesis. MFSD1 is a transporter protein that belongs to the major facilitator superfamily (MFS) and mainly mediates intestinal nutrient absorption, renal and hepatic clearance, metabolite transportation,[49] causing severe liver disease,[50] and average nutritional intake.[51] However, the biological functions of MFSD1 in pterygium development still need to be further illustrated. In addition to protein spectrum analysis, we also investigated whether U3 snoRNA affects the alteration of the transcriptome in pterygium cells, but we only found that a minimal number of gene transcription may be associated

Investigative Ophthalmology & Visual Science

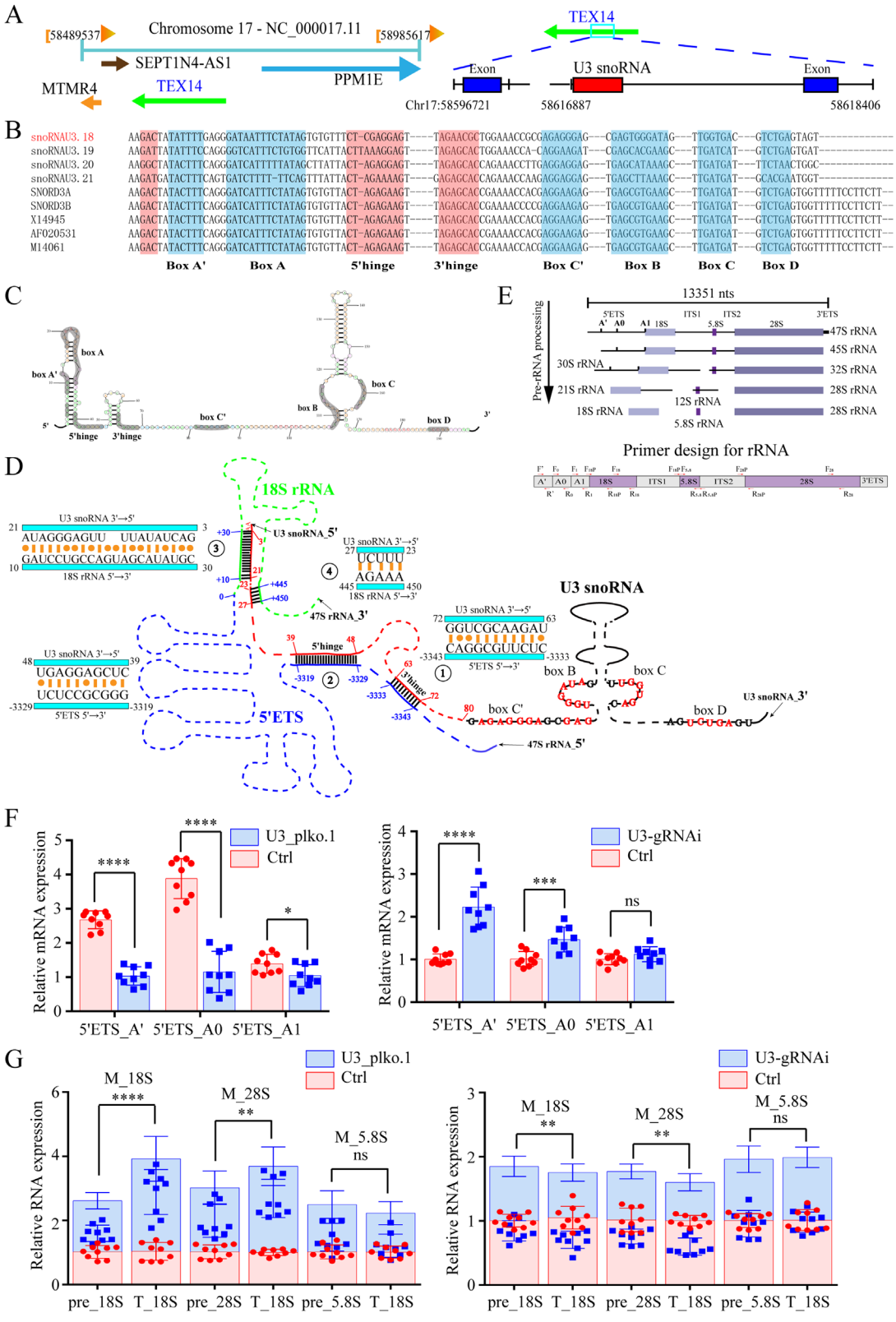

Figure 5. U3 snoRNA involves in the 47S rRNA shearing and maturation of 18S rRNA. (**A**) Host gene of U3 snoRNA in TEX14 gene on chromosome 17. (**B**) Determination of the structure of our atypical U3 snoRNA box through available U3 snoRNA (including three U3 snoRNAs [X14945, M14061, and AF020531]) in Rfam (version 14.7) and the SNORD3A reported in the study[53] as homology-based. (**C**) Spatial secondary structure of U3 snoRNA based on the structure on Ensembl. (**D**) Action site of atypical U3 snoRNA with precursor rRNA 47S rRNA. (**E**) Processing and primer design for precursor rRNA 47S rRNA and 18S rRNA, 28S rRNA, 5.8S rRNA. (**F**) Overexpression and knocking down of U3 snoRNA inhibited and promoted A′ and A0 in 5′ ETS, respectively. (**G**) Overexpression and knocking down of U3 snoRNA increased or decreased the maturity of 18S rRNA, respectively, even 28S rRNA generation (T_18S, T_28S, and T_5.8S represent total_18S, total_28S, and total_5.8S, respectively; M_18S, M_28S, and M_5.8S represent mature_18S, mature_28S, and mature_5.8S, respectively). *$P < 0.05$, **$P < 0.01$, ***$P < 0.001$, and ****$P < 0.0001$.

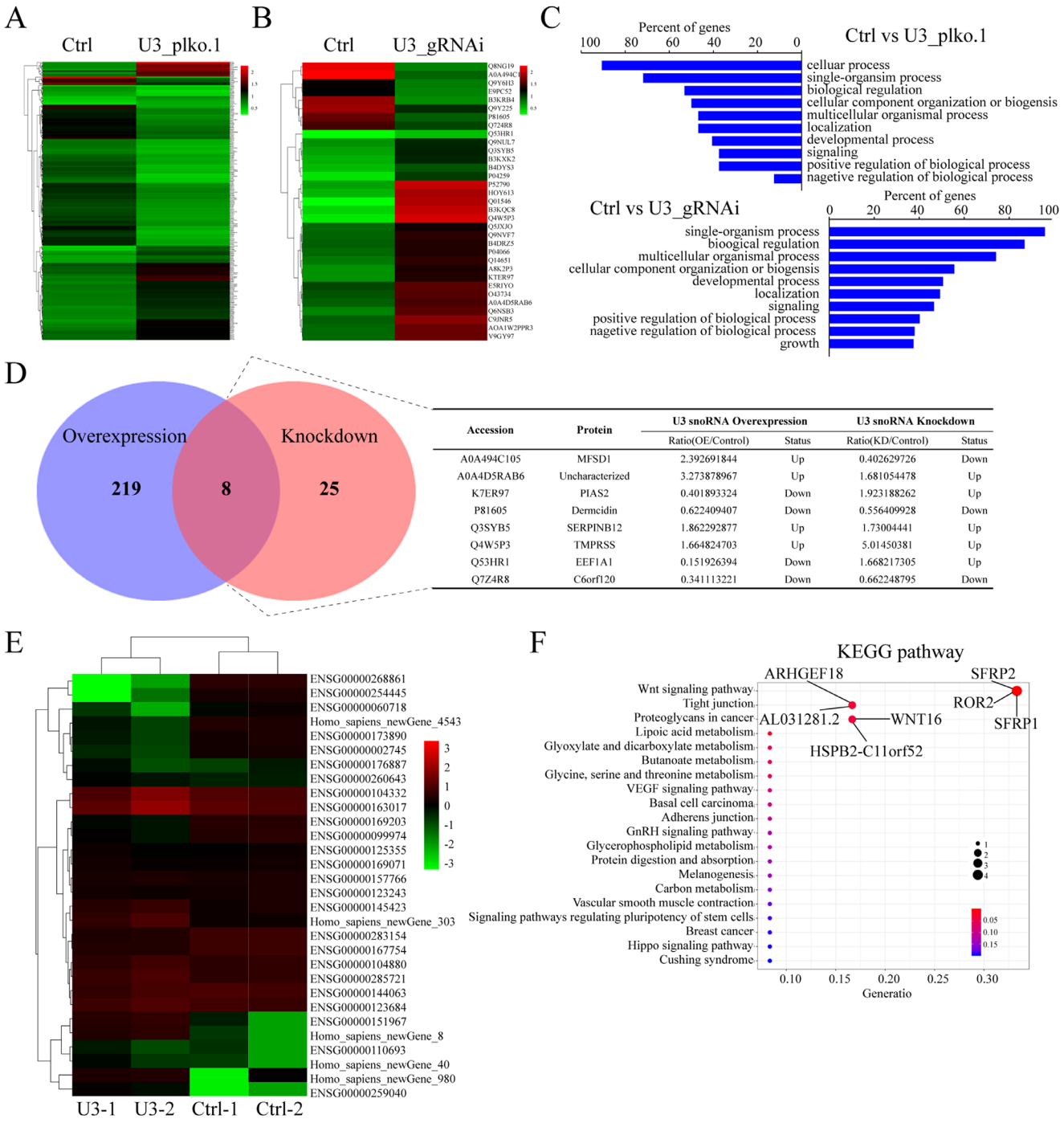

Accession	Protein	U3 snoRNA Overexpression		U3 snoRNA Knockdown	
		Ratio(OE/Control)	Status	Ratio(KD/Control)	Status
A0A494C105	MFSD1	2.392691844	Up	0.402629726	Down
A0A4D5RAB6	Uncharacterized	3.273878967	Up	1.681054478	Up
K7ER97	PIAS2	0.401893324	Down	1.923188262	Up
P81605	Dermcidin	0.622409407	Down	0.556409928	Down
Q3SYB5	SERPINB12	1.862292877	Up	1.73004441	Up
Q4W5P3	TMPRSS	1.664824703	Up	5.01450381	Up
Q53HR1	EEF1A1	0.151926394	Down	1.668217305	Up
Q7Z4R8	C6orf120	0.341113221	Down	0.662248795	Down

Figure 6. U3 snoRNA mainly affects the proteome profile by regulating the ribosome function in pterygium. (**A**) Heatmap of clustering depicting differentially expressed proteins in proteomic analysis of HPF overexpressing U3 snoRNA. (**B**) Heatmap of clustering presenting differentially expressed proteins in proteomic analysis of HCFs with knocked down U3 snoRNA. (**C**) Gene ontology (GO) process analysis of differential proteins in proteomic analysis of HPFs overexpressing U3 snoRNA and HCFs knocking down U3 snoRNA (biological processes section). (**D**) Venn diagram analysis of common differentially expressed proteins in HPFs overexpressing U3 snoRNA and HCFs knocking down U3 snoRNA. (**E**) Heatmap of differentially expressed genes in the transcriptomic analysis of HPF overexpressing U3 snoRNA in transcriptomics analysis. (**F**) Top 10 significantly enriched pathways of differential proteins in the transcriptomic analysis of HPFs overexpressing U3 snoRNA.

with U3 snoRNA and mainly involved in the Wnt signaling pathway (see Figs. 6E, 6F), which can cause cell epithelial-mesenchymal transition (EMT) and cell migration and is also essential for pterygium development.[52] More intriguingly, the gene transcripts of the screened differential proteins did not change significantly (see Table 2). Therefore, we speculated that the altered mRNA levels might result from specific protein actions. However, we do not exclude the potential function of U3 snoRNA in gene regulation in the development of pterygium.

Table 2. The mRNA Expression of the Eight Co-DEPs in HPFs Overexpressing U3 snoRNA and HCFs With Knocking Down U3 snoRNA

ID	Gene	Ctrl	Ctrl	U3_plko.1_1	U3_plko.1_2	*P* value	Control Average	OE Average	OE/Control
ENSG00000118855	MFSD1	33.508849	31.853827	31.714441	32.27386	0.5139	32.681338	31.784134	0.972546901
ENSG00000078043	PIAS2	7.12516	4.428562	6.731234	6.453167	0.6086	5.776861	5.579898	0.96590484
ENSG00000166634	SERPINB12	0	0	0	0	NA	0	0	NA
ENSG00000184012	TMPRSS2	0	0	0	0	NA	0	0	NA
ENSG00000087128	TMPRSS11E	0	0	0	0	NA	0	0	NA
ENSG00000137648	TMPRSS4	0	0	0	0	NA	0	0	NA
ENSG00000187045	TMPRSS6	0.011441	0.043308	0	0.021337	0.4755	0.0273745	0.021654	0.791028147
ENSG00000160183	TMPRSS3	0	0	0	0	NA	0	0	NA
ENSG00000186452	TMPRSS12	0	0	0	0	NA	0	0	NA
ENSG00000154646	TMPRSS15	0	0	0	0	NA	0	0	NA
ENSG00000198092	TMPRSS11F	0	0	0	0	NA	0	0	NA
ENSG00000137747	TMPRSS13	0	0	0	0	NA	0	0	NA
ENSG00000185873	TMPRSS11B	0	0	0	0	NA	0	0	NA
ENSG00000178297	TMPRSS9	0.094559	0.066113	0.151884	0.139489	0.0002	0.080336	0.1089985	1.356782762
ENSG00000187054	TMPRSS11A	0	0	0	0	NA	0	0	NA
ENSG00000176040	TMPRSS7	0.011408	0	0	0	0.4226	0.005704	0	0
ENSG00000166682	TMPRSS5	0.081229	0.056845	0.081063	0	0.57	0.069037	0.068954	0.998797746
ENSG00000153802	TMPRSS11D	0.019386	0	0	0	0.4226	0.009693	0	0
ENSG00000156508	EEF1A1	5390.287402	5796.613332	3801.660401	6020.48163	0.6067	5593.450367	4799.136867	0.857992214
ENSG00000185127	C6orf120	16.188618	14.097155	16.066051	14.566954	0.905	15.1428865	15.081603	0.995952984

NA, not applicable.

Conclusion

We report that suppressed U3 snoRNA in the pterygium promotes pterygium cell growth, proliferation, migration, and even cell cycle arrest. In the mechanism, U3 snoRNA in pterygium can bind to 5′ ETS of 47S rRNA and participate in the shearing of 5′ ETS in precursor rRNA (47S rRNA) and thereby the 18S rRNA maturation, which mainly causes protein alteration through affecting ribosome biosynthesis (see Fig. 7). This work reveals the functions and mechanisms of U3 snoRNA in developing pterygium. It explains how U3 snoRNA regulates ocular surface tissue homeostasis through epigenetic evolution, which provides a novel biology insight into pterygium and suggests potential perspective targets for pterygium precision therapy. However, we need to address the challenge that U3 snoRNA is mainly located in the nucleolus, which is hard for drug developing and targeting. Thus, we need to explore a deeper regulatory mechanism of U3 snoRNA to obtain a feasible target for therapy.

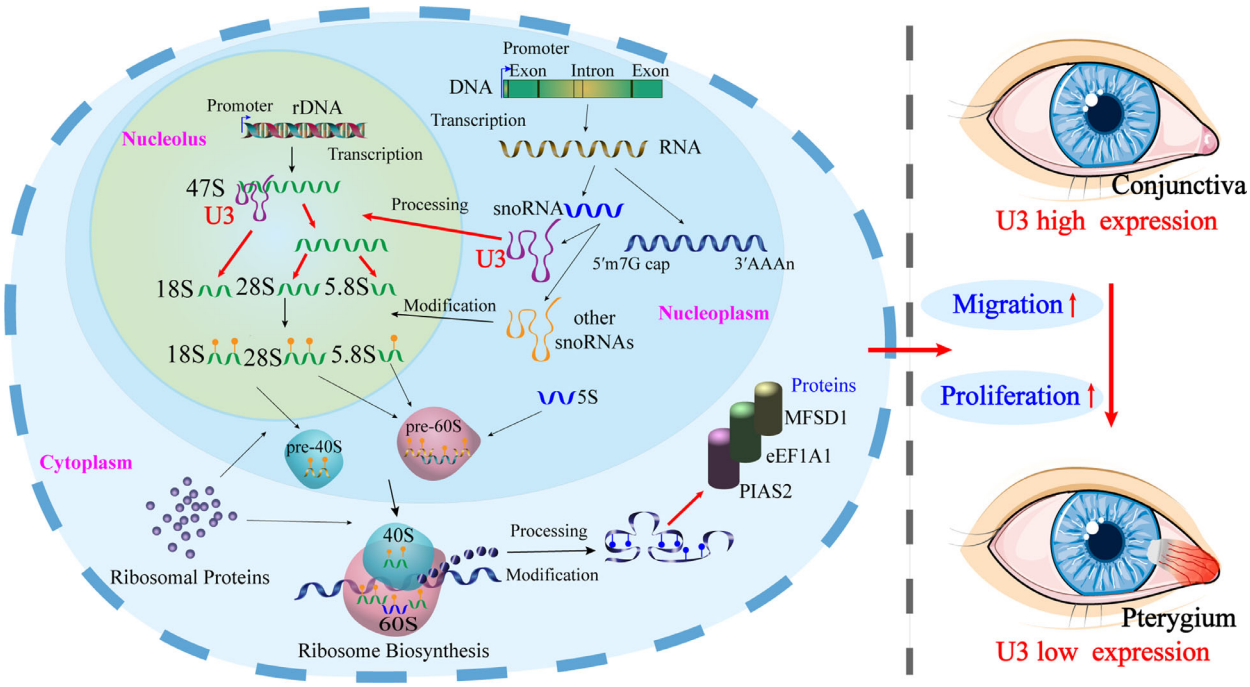

Figure 7. Graphic Abstract. U3 snoRNA functions on binding to the 5′ ETS and 18S rRNA in the precursor rRNA (47S rRNA) and promotes 18S rRNA maturation. U3 snoRNA involves in 40S ribosome function and ensures protein translation and synthesis. Once U3 snoRNA is suppressed in normal conjunctival fibroblasts or epidermal cells will lead to a delay of 18S rRNA maturation, ribosomal function deficiency, and aberrant protein synthesis, which may cause cell proliferation and migration changes, promoting the development of pterygium.

Investigative Ophthalmology & Visual Science

Data Availability

The RNA-seq and mass spectrum datasets supporting this study's findings have been deposited in the Gene Expression Omnibus (GEO) under the number GSE193086 and the ProteomeXchange with identifier PXD030801, respectively.

Acknowledgments

Supported by the Project of Key Disciplines of Medicine in Yangpu District of Shanghai (grant number YP19ZA01); the Project of Shanghai Yangpu District Science and Technology Commission, Health commission (grant number YPM202102); and the "Shanghai Morning Star Program" Sail Special (22YF1443100).

Author contributions: Y.C. and M.X. designed the work and prepared the manuscript. X.Z. collected the samples. X.Z., Y.J., W.A., and Q.W. performed the experiments, conducted data analyses, and wrote the manuscript. All authors discussed the results and read and approved the final version of the manuscript for publication.

Performed following the principles of the Declaration of Helsinki, and the study protocol was reviewed and approved by the Ethics Committee of Yangpu Hospital. Informed consent was provided by all subjects enrolled in this study. The ethical approval number is LL-2018-WSJ-010.

Disclosure: **X. Zhang,** None; **Y. Jiang,** None; **Q. Wang,** None; **W. An,** None; **X. Zhang,** None; **M. Xu,** None; **Y. Chen,** None

References

1. Wan Zaki WMD, Mat Daud M, Abdani SR, Hussain A, Mutalib HA. Automated pterygium detection method of anterior segment photographed images. *Comput Methods Programs Biomed*. 2018;154:71–78.
2. Chu WK, Choi HL, Bhat AK, Jhanji V, *Pterygium: New Insights. Eye (Lond)*. 2020;34:1047–1050.
3. Young AL, Cao D, Chu WK, et al . The Evolving Story of Pterygium. *Cornea*. 2018;37(Suppl 1):S55–S57.
4. Rezvan F, Khabazkhoob M, Hooshmand E, Yekta A, Saatchi M, Hashemi H. Prevalence and risk factors of pterygium: a systematic review and meta-analysis. *Surv Ophthalmol*. 2018;63:719–735.
5. Janson BJ, Sikder S. Surgical management of pterygium. *Ocul Surf*. 2014;12:112–119.
6. Nuzzi R, Tridico F. How to minimize pterygium recurrence rates: clinical perspectives. *Clin Ophthalmol*. 2018;12:2347–2362.
7. Shahraki T, Arabi A, Feizi S. Pterygium: an update on pathophysiology, clinical features, and management. *Ther Adv Ophthalmol*. 2021;13:25158414211020152.
8. Wu M, Wang S, Wang Y, Zhang F, Shao T. Targeted delivery of mitomycin C-loaded and LDL-conjugated mesoporous silica nanoparticles for inhibiting the proliferation of pterygium subconjunctival fibroblasts. *Exp Eye Res*. 2020;197:108124.
9. Reisman D, McFadden JW, Lu G. Loss of heterozygosity and p53 expression in Pterygium. *Cancer Lett*. 2004;206:77–83.
10. Tsai YY, Chang CC, Chiang CC, et al . HPV infection and p53 inactivation in pterygium. *Mol Vis*. 2009;15:1092–1097.
11. Wu CW, Peng ML, Yeh KT, Tsai YY, Chiang CC, Cheng YW. Inactivation of p53 in pterygium influence miR-200a expression resulting in ZEB1/ZEB2 up-regulation and EMT processing. *Exp Eye Res*. 2016;146:206–211.
12. Li W, Liu J, Galvin JA. Epigenetics and Common Ophthalmic Diseases. *Yale J Biol Med*. 2016;89:597–600.
13. Lanza M, Benincasa G, Costa D, Napoli C. Clinical Role of Epigenetics and Network Analysis in Eye Diseases: A Translational Science Review. *J Ophthalmol*. 2019;2019:2424956.
14. Turi Z, Lacey M, Mistrik M, Moudry P. Impaired ribosome biogenesis: mechanisms and relevance to cancer and aging. *Aging (Albany NY)*. 2019;11:2512–2540.
15. Iouk TL, Aitchison JD, Maguire S, Wozniak RW. Rrb1p, a yeast nuclear WD-repeat protein involved in the regulation of ribosome biosynthesis. *Mol Cell Biol*. 2001;21:1260–1271.
16. Ojha S, Malla S, Lyons SM. snoRNPs: Functions in Ribosome Biogenesis. *Biomolecules*. 2020;10:783.
17. Watkins NJ, Ségault V, Charpentier B, et al . A common core RNP structure shared between the small nucleoar box C/D RNPs and the spliceosomal U4 snRNP. *Cell*. 2000;103:457–466.
18. Liang J, Wen J, Huang Z, Chen XP, Zhang BX, Chu L. Small Nucleolar RNAs: Insight Into Their Function in Cancer. *Front Oncol*. 2019;9:587.
19. Bratkovič T, Božič J, Rogelj B. Functional diversity of small nucleolar RNAs. *Nucleic Acids Res*. 2020;48:1627–1651.
20. Yoshihama M, Nakao A, Kenmochi N. snOPY: a small nucleolar RNA orthological gene database. *BMC Res Notes*. 2013;6:426.
21. Kiss AM, Jády BE, Bertrand E, Kiss T. Human box H/ACA pseudouridylation guide RNA machinery. *Mol Cell Biol*. 2004;24:5797–5807.
22. Lafontaine DL. Noncoding RNAs in eukaryotic ribosome biogenesis and function. *Nat Struct Mol Biol*. 2015;22:11–19.
23. Chen J, Zhang L, Ye K. Functional regions in the 5' external transcribed spacer of yeast pre-rRNA. *Rna*. 2020;26:866–877.
24. Chen Y, Wang H, Jiang Y, Zhang X, Wang Q. Transcriptional profiling to identify the key genes and pathways of pterygium. *PeerJ*. 2020;8:e9056.
25. Jiang Y, Zhang X, Zhang X, et al . Comprehensive Analysis of the Transcriptome-Wide m6A Methylome in Pterygium by MeRIP Sequencing. *Front Cell Dev Biol*. 2021;9:670528.
26. Fujita Y, Khateb A, Li Y, et al . Regulation of S100A8 Stability by RNF5 in Intestinal Epithelial Cells Determines Intestinal Inflammation and Severity of Colitis. *Cell Rep*. 2018;24:3296–3311.e6.
27. Ran FA, Hsu PD, Wright J, Agarwala V, Scott DA, Zhang F. Genome engineering using the CRISPR-Cas9 system. *Nat Protoc*. 2013;8:2281–2308.
28. Chen K, Lai K, Zhang X, et al . Bromfenac Inhibits TGF-beta1-Induced Fibrotic Effects in Human Pterygium and Conjunctival Fibroblasts. *Invest Ophthalmol Vis Sci*. 2019;60:1156–1164.
29. Liu L, Michowski W, Kolodziejczyk A, Sicinski P. The cell cycle in stem cell proliferation, pluripotency and differentiation. *Nat Cell Biol*. 2019;21:1060–1067.
30. Hughes JM, Ares M, Jr. Depletion of U3 small nucleolar RNA inhibits cleavage in the 5′ external transcribed spacer of yeast pre-ribosomal RNA and impairs formation of 18S ribosomal RNA. *Embo J*. 1991;10:4231–4239.
31. Abraham KJ, Khosraviani N, Chan JNY, et al . Nucleolar RNA polymerase II drives ribosome biogenesis. *Nature*. 2020;585:298–302.
32. Shibata N, Ishida H, Kiyokawa E, Singh DP, Sasaki H, Kubo E. Relative gene expression analysis of human pterygium tissues and UV radiation-evoked gene expression patterns in corneal and conjunctival cells. *Exp Eye Res*. 2020;199:108194.
33. Kim SW, Kim HI, Thapa B, Nuwormegbe S, Lee K. Critical Role of mTORC2-Akt Signaling in TGF-β1-Induced Myofi-

broblast Differentiation of Human Pterygium Fibroblasts. *Invest Ophthalmol Vis Sci*. 2019;60:82–92.
34. Ishioka M, Shimmura S, Yagi Y, Tsubota K. Pterygium and dry eye. *Ophthalmologica*. 2001;215:209–211.
35. Chui J, Di Girolamo N, Wakefield D, Coroneo MT. The pathogenesis of pterygium: current concepts and their therapeutic implications. *Ocul Surf*. 2008;6:24–43.
36. Di Girolamo N, Chui J, Coroneo MT, Wakefield D. Pathogenesis of pterygia: role of cytokines, growth factors, and matrix metalloproteinases. *Prog Retin Eye Res*. 2004;23:195–228.
37. Zada M, Pattamatta U, White A. Modulation of Fibroblasts in Conjunctival Wound Healing. *Ophthalmology*. 2018;125:179–192.
38. Chen E, Bohm K, Rosenblatt M, Kang K. Epigenetic regulation of anterior segment diseases and potential therapeutics. *Ocul Surf*. 2020;18:383–395.
39. Alkozi HA, Franco R, Pintor JJ. Epigenetics in the Eye: An Overview of the Most Relevant Ocular Diseases. *Front Genet*. 2017;8:144.
40. He S, Huang Y, Dong S, et al . MiR-199a-3p/5p participated in TGF-β and EGF induced EMT by targeting DUSP5/MAP3K11 in pterygium. *J Transl Med*. 2020;18:332.
41. Xu N, Cui Y, Dong J, Huang L. Exploring the Molecular Mechanisms of Pterygium by Constructing lncRNA-miRNA-mRNA Regulatory Network. *Invest Ophthalmol Vis Sci*. 2020;61:12.
42. Zhang C, Hu J, Yu Y. CircRNA Is a Rising Star in Researches of Ocular Diseases. *Front Cell Dev Biol*. 2020;8:850.
43. Kiss T. Small nucleolar RNAs: an abundant group of noncoding RNAs with diverse cellular functions. *Cell*. 2002;109:145–148.
44. Hunziker M, Barandun J, Petfalski E, et al . UtpA and UtpB chaperone nascent pre-ribosomal RNA and U3 snoRNA to initiate eukaryotic ribosome assembly. *Nat Commun*. 2002;7(2016):12090.
45. Peña C, Hurt E, Panse VG. Eukaryotic ribosome assembly, transport and quality control. *Nat Struct Mol Biol*. 2017;24:689–699.
46. Baßler J, Hurt E. Eukaryotic Ribosome Assembly. *Annu Rev Biochem*. 2019;88:281–306.
47. Clerget G, Bourguignon-Igel V, Marmier-Gourrier N, et al . Synergistic defects in pre-rRNA processing from mutations in the U3-specific protein Rrp9 and U3 snoRNA. *Nucleic Acids Res*. 2020;48:3848–3868.
48. Mullineux ST, Lafontaine DL. Mapping the cleavage sites on mammalian pre-rRNAs: where do we stand? *Biochimie*. 2012;94:1521–1532.
49. Quistgaard EM, Löw C, Guettou F, Nordlund P. Understanding transport by the major facilitator superfamily (MFS): structures pave the way. *Nat Rev Mol Cell Biol*. 2016;17:123–132.
50. Massa López D, Thelen M, Stahl F, et al . The lysosomal transporter MFSD1 is essential for liver homeostasis and critically depends on its accessory subunit GLMP. *Elife*. 2019;8:e50025.
51. Perland E, Hellsten SV, Lekholm E, Eriksson MM, Arapi V, Fredriksson R. The Novel Membrane-Bound Proteins MFSD1 and MFSD3 are Putative SLC Transporters Affected by Altered Nutrient Intake. *J Mol Neurosci*. 2017;61:199–214.
52. Shu DY, Lovicu FJ. Myofibroblast transdifferentiation: The dark force in ocular wound healing and fibrosis. *Prog Retin Eye Res*. 2017;60:44–65.
53. Lemus-Diaz N, Ferreira RR, Bohnsack KE, Gruber J, Bohnsack MT. The human box C/D snoRNA U3 is a miRNA source and miR-U3 regulates expression of sortin nexin 27. *Nucleic Acids Res*. 2020;48:8074–8089.

Investigative Ophthalmology & Visual Science